46. ORGANIC MATTER IN LEG 96 SEDIMENTS: CHARACTERIZATION BY PYROLYSIS[1]

Jean K. Whelan and Martha Tarafa, Woods Hole Oceanographic Institution[2]

ABSTRACT

Sediments from Deep Sea Drilling Project Sites 615, 617, 618, 619, and 620–623 were subjected to pyrolysis. The sediments are immature with respect to petroleum generation as determined by production index values of less than 0.1 and T_{max} values of 460–480°C. The amount of pyrolyzable organic matter was moderately low as compared to typical petroleum source rocks. The immature organic matter present does not appear to contain a significant proportion of woody material as shown by the low gas-generating potential. Typical overbank sediments from Sites 617 and 620 generally show higher P_2 values (500–800 μg hydrocarbon per g dry weight sediment) than typical channel-fill sediments from Sites 621 and 622 (P_2 = 450–560 μg/g). T_{max} for both types of sediment remained very constant (462–468°C) with a slight elevation (+15°C) occurring in samples containing lignite. The highest P_2 values occurred in sections described as turbidites. Very low P_2 values (about 50 μg/g) occurred in sands. P_2 values for shallower sections of basin Sites 618 and 619 tended to be higher (900–1000 μg/g) and decreased in deeper, more terrigenous sections of Site 619. Preliminary experiments indicate that microbiological degradation of sediment organic matter causes a decrease in P_2. Pyrolyzable organic matter from lower fan Site 623 appears to increase with depth in two different sediment sequences (40–85 and 95–125 m sub-bottom). Organic matter type, as shown by pyrolysis capillary gas chromatography (GC) patterns, was generally the same throughout the well, with much more scatter occurring in the deepest sections (130–155 m sub-bottom). One major and two minor organic matter types could be recognized in both fan and basin sites drilled on Leg 96.

INTRODUCTION

Thermal techniques are now used routinely for determining the amount of petroleum produced and the petroleum-generation potential of source rocks (Espitalié et al., 1977; Claypool and Reed, 1976; Huc and Hunt, 1980; Barker, 1974; Dembicki et al., 1983). These techniques were applied in this study to immature marine sediments to examine high molecular weight organic material and to correlate pyrolysis properties with other geological characteristics. The rationale for using these measurements on immature and surface sediments was that pyrolysis gives a measure of hydrogen-rich (reduced) organic matter in a sample (Espitalié et al., 1977). Analysis of this material could provide information on the source and early diagenetic history of the sediment which might be a useful paleontological tool.

Hydrogen-rich organic material can be lost from sediments in either of two general ways: (1) thermally (in the petroleum-generating process) or (2) by biological degradation which normally accompanies sediment reworking—such as that which occurs under oxic conditions in the water column or at the sediment/water interface. Rapidly buried sediments would be removed more quickly from this oxic zone where rapid biodegradation could occur and, therefore, should contain a higher content of pyrolyzable organic matter than more slowly deposited sediments (assuming bottom-water oxygen conditions remain constant). In addition, higher temperatures might be required to break down more reworked (hydrogen-poor) organic matter. These ideas were tested on Deep Sea Drilling Project (DSDP) Leg 95 sediments (Tarafa, Whelan, and Mountain, in press) and by subjecting sediments from DSDP Leg 96 (Gulf of Mexico including the lower Mississippi Fan) to pyrolysis analyses as described below. In addition, preliminary laboratory experiments were carried out to determine whether microbiological degradation can cause a decrease in pyrolyzable organic matter.

METHODS

Wet sediment was ground with a mortar and pestle and 50–100 mg samples were placed in a quartz tube, held in place with quartz wool, and pyrolyzed by procedures previously described in detail (Whelan et al., 1983). Briefly, the samples were placed in a desorption probe in the cooled interface of a Chemical Data Systems (CDS) Model 820 Geological Reaction System and heated at 40°C per minute from 200 to 500°C. Organic compounds desorbed during the heating process were swept out of the system in a helium stream. The stream was split with part going directly to a flame ionization detector. During the heating process, the compounds evolved by heating elute as two peaks—the lower temperature peak (P_1) evolving at 150–250°C represents sorbed organic compounds naturally present in the sediment; the higher temperature peak (P_2) evolving at 400–500°C represents compounds cracked from (thermally broken off) the sediment kerogen or protokerogen (high molecular weight organic) matrix. The temperature maximum of this peak, called T_{max}, is measured via a thermocouple placed next to the sediment sample. It should be noted that this procedure gives somewhat different absolute T_{max} values than (but the same profile as) the more commonly used Rock Eval apparatus (J. K. Whelan, K. Peters, and M. E. Tarafa, unpublished results). Profiles of P_1, P_2, and T_{max} as a function of depth are shown in Figure 3 for the extensive suite of Site 623 samples analyzed in this work. Error bars show 1σ standard deviations for replicate grinds. Error bars for duplicate samples taken from the same grind (not shown) were generally smaller than the width of the data points. The production index (PI), $P_1/(P_1 + P_2)$, is also shown. This is a parameter commonly used in petroleum source rock analysis which gives the ratio of generated to total petroleum-generating potential of the sediment (Espitalié et al., 1977).

The pyrolyzed material evolved in P_2 was also trapped and analyzed by capillary GC in some cases, as shown in Figures 4 and 5.

Carbon content was determined by combustion, using a Leco Apparatus. Organic carbon was determined on ground, dried, and decarbonated (by HCl vapor) samples (Whelan et al., 1984).

[1] Bouma, A. H., Coleman, J. M., Meyer, A. W., et al., *Init. Repts. DSDP*, 96: Washington (U.S. Govt. Printing Office).

[2] Address: (Whelan, Tarafa) Chemistry Department, Woods Hole Oceanographic Institution, Woods Hole, MA 02543.

RESULTS AND DISCUSSION

General

The production index values (PI) of sediments examined in this work are all less than 0.1, which shows that they are immature with respect to petroleum generation and cannot contain more than traces of migrated petroleum. The latter conclusion differs from that of Kennicutt et al. (this volume), who conclude that migrated hydrocarbons are generally present in fan and basin sediments. These authors base their conclusions on qualitative (rather than quantitative) data consisting of solvent extraction hydrocarbon compositions. These solvent extractable hydrocarbons correspond to the P_1 components in the current work (representing levels of hydrocarbons naturally present in the sediments) which are low and fairly constant throughout all samples ranging from about 10 to 20 ppm. These low levels are more consistent with a source from recycled terrigenous sediments than from migrated petroleum. Kennicutt et al. (this volume) point out that these two alternatives cannot be distinguished from their data.

In contrast, P_2 values, reflecting the potential of organic matter in the sediment for generating hydrocarbons if subjected to further burial and higher temperatures, is more variable. The P_2 values are generally on the low side for samples from all sites as compared to a typical good petroleum source rock (Table 1) ranging from about 50 to 800 for fan sites and from 300 to 1000 for basin sites. For comparison, values from a number of Alaskan North Slope wells, classified as having low to moderate generating potential, fall in the 200–2000 ppm range (Claypool and Magoon, 1985).

Fan Sites 615, 617, 620, 621, and 622

A few samples from characteristic fan sediments were analyzed in order to determine if pyrolyzable organic matter (P_2) and T_{max} differed between channel-fill and overbank sediments. (P_1 values were usually very low and are, therefore, generally not reported.) P_2 and T_{max} values were obtained from midfan sites for representative overbank sequences from Sites 617 and 620, and from representative channel-fill sequences from Sites 621 and 622 (Table 1). In addition, a number of samples were also examined from lower fan Sites 615 and 623 where overbank and channel sequences are not as well defined and tend to interbed (Coleman, Bouma, et al., this volume). Bottom sections of Site 615 represented the oldest sediments recovered on this leg. A very extensive suite of Site 623 samples were analyzed, as discussed in a separate section.

For samples containing only silt and mud (and no sand), the midfan overbank sediments (indicated as OB from Sites 617 and 620) generally show significantly higher P_2 values (540 to 800 μg/g or ppm) than the midfan channel-fill sequences (P_2 = 450–560 μg/g from Sites 621 and 622 indicated by CF in Table 1). T_{max} values for both types of samples are very constant (462–468°C). Exceptions appear to occur in samples containing small amounts of lignite, such as Sample 622-6-1, 50–51 cm which shows T_{max} to be higher by about 15°C with more scatter in replicate values. This sample also shows a slightly lower P_2 (possibly resulting from greater reworking of the organic matter) than found for the other two samples from this site.

In addition, P_2 also appears to vary with grain size with sections containing sands showing much lower values than those with only mud or silty mud (Table 1). For example, Samples 615-3-3, 8–9 cm, and 615-5-3, 99–100 cm, which are sands or silty sands, both show very low P_2 values (57 and 63 μg/g, respectively), as compared to Samples 615-3-2, 30–31 cm and 615-3-3, 63–64 cm, which are muds or silty muds and have P_2 values almost an order of magnitude higher (637 and 624 μg/g, respectively). This difference is much larger than that between channel fill and overbank sites which was described above. No consistent difference is observable between muds and silts. For example, P_2 values for overbank samples from Site 620, which are generally homogeneous clays, show almost the same P_2 values as overbank sediments from Site 617, which generally contain a small amount of silt as well. T_{max} values for all of these sections remain very constant (except for those containing lignite as discussed above).

Several slightly elevated P_2 values appear to correlate with sections described as turbidites. Examples include Samples 615-33-1, 46–47 cm (P_2 = 773 μg/g as compared to values for silty muds in the rest of the hole of about 600) and Sample 617-5-4, 49–50 cm (867 μg/g as compared to other Site 617 values generally around 700 μg/g). These examples are similar to results from Leg 95, where it was found that high P_2 values could be used to identify turbidites or slumps in some cases (Tarafa et al., in press).

It should also be noted that P_2 values tend to decrease somewhat (compared to the two samples just discussed) at the bottom of Site 615 (below 485 m) in a more marine section containing redeposited carbonates (Kohl et al., this volume).

Sites 619 and 618

Sediments from the two basin sites which contain more hemipelagic sediments than the fan sites were also investigated (Table 1 and Figures 1 and 2). P_2 values for shallower sections of both these holes are generally higher than for any of the Mississippi Fan sections. For example, values range from about 900 to 1000 μg/g from 28 to 73 m sub-bottom at Site 619 with the surface (4 m) and deeper sections (below 78 m) having values more comparable to those of the fan sediments. The deeper lower values (generally less than 500 μg/g below 110 ft. sub-bottom) correlate with sediments in which methane gas (and possibly microbiological methanogenic activity) was found (Whelan et al., this volume). However, some of the sections containing particularly low P_2 values as compared to other values for this site (such as Samples 619-13-4, 130–150 cm and 619-17-3, 130 cm with P_2 values of 414 and 343 μg/g, respectively) were also burrowed or bioturbated (Table 1, Bouma, Stelting et al., this volume).

The deeper sections of Site 619 below 100 m sub-bottom, where P_2 values decrease, may also contain a larger

Table 1. Summary of pyrolysis data and lithology for Leg 96 samples.

Core-Section (level or interval in cm)	Sub-bottom depth (m)	Type[a]	P_2[b,c] (μg/g)	T_{max}[b] (°C)	Description of sediment
Hole 615					
3-2, 30–31	13.90		637 ± 91	463 ± 2.8	Mud with silt; laminated
3-2, 70–71	14.30		571 ± 331	470	Dark grey sandy silt; laminated
3-2, 72	14.32		1002	475 ± 1.4	Dark grey sandy silt; laminated
3-2, 93	14.53		45	455	Dark grey sandy silt; laminated
3-3, 8–9	15.18		57 ± 2	454 ± 12	Silty sand — fining upward sequence?
3-3, 63–64	15.73		624 ± 3	463 ± 2.8	Silty mud
5-3, 99–100	33.59		63 ± 1.7	464 ± 9.2	Silty sand
5-4, 40–41	34.50		241 ± 110	470 ± 6.4	Mud with deformed silty layers
6-4	43.60		783	467 ± 1	Dark grey silt-sand (drilling disturbance)
6-5, 120–121	46.30		668 ± 471	463 ± 2.8	Muddy silt — fine-grained turbidite
6-6, 10–11	46.70		139 ± 15	464 ± 4.2	Sorted silty sand
9-1, 77	68.00		474 ± 11	471 ± 7	Silt laminated mud
9-3, 0–2	70.20		276	478 ± 5	Silty sand
10-1, 10–11	76.80		701 ± 89	461 ± 1.4	Silty mud
10-1, 58–59	77.28		177 ± 13	470 ± 3.5	Silty sand (with chert and lignite)
33-1, 46–47	305.16		773 ± 83	468.5 ± 0.71	Silty turbidite mud
47-2, 42–43	458.62		600 ± 42	471.5 ± 2.1	Silty mud in layers with lignite
49-1, 2–3	485.22		437 ± 52	467 ± 2.8	Nannofossil ooze (homogeneous)
50-1, 3–4	494.73		575 ± 7.6	467 ± 2.8	Nannofossil ooze
51-1, 5–6	504.25		599 ± 40	464.5 ± 6.4	Foraminifer nannofossil ooze
Hole 617					
1-3, 23–24	3.23	OB	701 ± 56	465 ± 1.4	Rapid nephloid sedimentation
3-1, 28–29	17.88	OB	678 ± 59	462 ± 1.4	Slump on back side of levee
5-4, 49–50	41.79	OB	867 ± 37	462.5 ± 3.5	Silty mud turbidite on levee
8-1, 49–50	65.79	OB	695 ± 31	463.5 ± 2.8	Mud with silt laminae
11-4, 41–42	99.01	OB	540 ± 92	462 ± 5.2	Mud with silt laminae; fine-grained turbidite
Average			696 ± 116		
Hole 618					
10-2, 40	81.00		591 ± 48	nd[d]	Dark grey homogeneous (?) mud
Hole 618A					
1, top	9.20		1061 ± 23	nd	Dark green-grey homogeneous mud
1-2, 13	10.82		500	480 ± 2.8	Dark green-grey mud
1-4, 130–150	15.00		930 ± 139	nd	Very dark mud — gassy
1-5, 130–150	16.50		625 ± 82	nd	Very dark mud — gassy
2-5, 0–20	34.00		462 ± 51	nd	Dark grey mud with black blebs
3-4, 2–80	40.00		702 ± 273	nd	Dark grey gassy mud — grey blebs
Hole 619					
1-2, 13	2.63		401	nd	Dark grey mud — bioturbated — thin silt laminae
1-2, 130–150	4.00		523 ± 206	nd	Dark grey mud — bioturbated — thin silt laminae
4-5, 130–150	28.00		929 ± 129	nd	Laminated dark mud with streaks
5-4, 130–150	36.00		1672 ± 219	nd	Dark grey laminated mud
6-5, 130–150	47.00		1027 ± 59	nd	Dark grey homogeneous mud
7-5, 129	57.00		872 ± 27	nd	Dark grey mud with laminae?
8-4, 130–150	65.00		1033 ± 31	nd	Dark grey laminated mud
9-3, 95	72.65		939 ± 105	nd	Dark grey laminated mud
10-4, 124	78.00		744 ± 74	nd	Dark grey laminated gassy mud
11-3, 130–150	92.00		731 ± 57	nd	Dark grey laminated mud
12-3, 105	102.00		540 ± 37	nd	Dark grey homogeneous gassy mud
13-4, 130–150	113.00		414 ± 60	nd	Dark grey burrowed mud
14-2, 44	119.00		688 ± 25	nd	Dark grey homogeneous mud
16-4, 83	141.00		444 ± 55	nd	Dark green-grey mud — silt laminated?
17-3, 130–150	150.00		343 ± 30	nd	Bioturbated mud — reworked clasts
19-2, 120–150	167.00		419 ± 28	nd	Mud with silt and sand layers
Hole 620					
2-1, 41–42	3.41	OB	689 ± 103	464 ± 6.4	Clay (homogeneous)
7-1, 50–51	51.50	OB	587 ± 27	468 ± 4.2	Clay (drilling disturbance)
Average			638 ± 72		
Hole 621					
2-1, 50–51	4.00	CF	457 ± 42	466 ± 1.4	Clay with dark organic-rich zones
5-1, 50–51	32.80	CF	497 ± 32	468 ± 1.4	Dark grey mud (homogeneous)
7-1, 50–51	46.70	CF	541 ± 35	468 ± 9.2	Dark grey mud (gas pockets)
Average			498 ± 42		
Hole 622					
2-1, 50–51	4.00	CF	543 ± 16	464 ± 2.8	Dark grey mud — laminae?
6-1, 50–51	42.20	CF	477 ± 23	482 ± 8.4	Dark grey — lignite-gas
8-1, 50–51	61.30	CF	545 ± 35	466 ± 2.8	Dark grey — homogeneous
Average			522 ± 39		

[a] OB = overbank; CF = channel fill as identified by Stelting et al. (this volume).
[b] 1σ standard deviations are shown.
[c] μg hydrocarbon per g dry wt. sediment.
[d] nd = not determined.

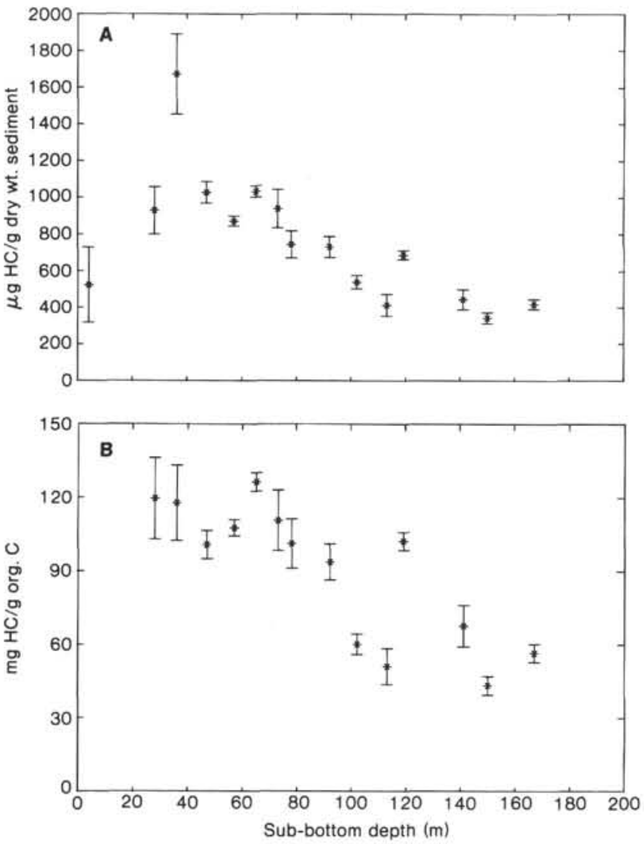

Figure 1. A. Pyrolysis P_2 yields for Hole 619A (μg hydrocarbon/g dry wt. sediment). B. Pyrolysis P_2 yields for Hole 619 (mg hydrocarbon/g organic carbon).

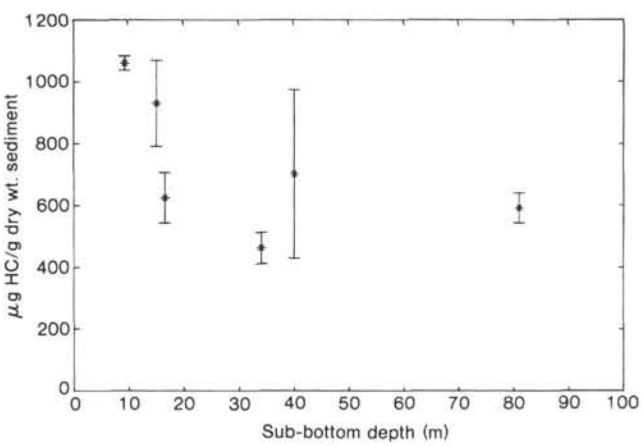

Figure 2. Pyrolysis P_2 yields for Site 618 (μg hydrocarbon/g dry wt. sediment).

proportion of terrigenous organic matter as suggested by increases in terrigenous over marine lipid biomarkers (such as lower n-C_{17}/n-C_{29} ratios and higher odd–even preference index [OEPI] values, Requejo et al., this volume). This decrease in P_2 is not accompanied by a corresponding decrease in organic carbon which remains relatively constant at about 0.7–0.8% throughout the hole (Whelan et al., this volume). To test this point further, a plot of P_2 normalized to organic carbon is shown in Figure 1B and, except for one elevated point at 119 m, also exhibits a sharp decrease below 100 m sub-bottom.

Site 618 sediments produce more scatter in P_2 values (Table 1 and Fig. 2). For example, an exponential(?) decrease in P_2 values occurs between 15 and 16.5 m, even though these two samples are from the same core, which visually consisted of the same homogeneous dark gray gassey mud.

Two of the shallowest Site 618 sections with P_2 values of 930 and 1060 μg/g are comparable to those of the richer sections from Site 619. The rapid P_2 decrease below 15 m may be real and related to the sharp increase in core gas microbiological methane which occurs in the same interval (Whelan et al., this volume). Alternatively, this scatter could be a result of sediment heterogeneity caused by surface slumping (see Site 619 chapter).

Effect of Microbiological Degradation on P_2

Some very preliminary experiments were carried out to test effects of microbiological degradation on P_2. An aliquot of sediment from the top of Site 618 was allowed to stand in a covered beaker at room temperature on the bench top for several months. A portion was analyzed periodically for P_2 as shown in Table 2. It can be seen that a significant decrease in pyrolyzable organic matter occurred over the course of the experiment with the largest decrease occurring during the first 7 days of the experiment. Because of the preliminary nature of the experiment, no attempt was made either to exclude air from the sediment or to mix it well with air to avoid development of anaerobic zones. Thus, the organisms causing the P_2 decrease could have been either aerobes or anaerobes or a combination of both. Experiments are now in progress to see if similar decrease can be observed under strict anaerobic conditions. For purposes of the current work, the experiment does show that microbiological degradation either at or shortly after sediment deposition could have caused the observed changes in P_2 in both Leg 96 sediments, as discussed above, and in Leg 95 sediments (Tarafa et al., in press).

Site 623

Results from pyrolysis of Site 623 samples are shown in Table 3 and Figure 3. There appears to be a small decrease in P_2 with depth from 10 to 25 m. A gradual increase then occurs from about 40 to 85 m sub-bottom where error bars on replicate samples (separate grinds, see Methods section) are approximately the width of the

Table 2. Changes in pyrolyzable carbon (P_2) and T_{max} in sediment (618A, top) left standing in covered container at room temperature for time indicated.

Time (days)	$P_2 \pm 1\sigma$ standard deviation (μg hydrocarbon/g dry wt. sediment)	T_{max} (°C)
0	607 ± 10 (duplicate samples)	456–461
7	503	n.d.[a]
38	482 ± 18 (triplicate)	466–470
76	396 ± 13 (duplicate)	n.d.
137	410 ± 5 (duplicate)	470–473

[a] n.d. = not determined.

Table 3. Summary of pyrolysis P_2 capillary GC patterns and percentage organic carbon for Leg 96 sediments.

Core-Section (level or interval in cm)	Sub-bottom depth (m)	Organic C (%)	P_2 capillary GC pattern[a]	PI	P_2[b]	T_{max} (°C)
Hole 623						
2-2, 115	9.2	n.d.[c]	A	0.034	479	470
2-3, 45	10.0	n.d.	A	0.034	556	469
3-1, 45–47	n.d.	1.31	n.d.	n.d.	n.d.	n.d.
3-1, 115	16.2	1.31	A	0.045	485	462
3-5, 45	22.6	n.d.	A	0.062	351	470
5-2, 115	38	1.06	A	0.044	425	465
6-3, 115	49.2	n.d.	A	0.039	440	466
7-2, 42		1.12	n.d.	n.d.	n.d.	n.d.
8-2, 69	66.4	n.d.	A	0.032	545	464
9-2, 43	75.7	1.03	B	0.055	662	464
10-3, 3–6	86.4	n.d.	A	0.029	481	472
11-3, 1–3	97.0	0.97	A	0.040	350	472
12-1, 1–37	103	n.d.	A	0.058	471	464
12-3, 91–93	105.6	0.86	n.d.	n.d.	n.d.	n.d.
12-4, 17	107.3	n.d.	A	0.026	473	468
12-4, 110	108.2	n.d.	A	0.040	423	468
13-1, 7	112.2	1.16	A	0.029	614	468
14-2, 98	123.9	1.27	A	0.023	664	462
14-3, 50	124.9	n.d.	B	0.049	805	468
15-1, 17–19	131	n.d.	C	0.103	51	475
15-1, 98	131.8	n.d.	D	0.058	161	479
16-1, 45	140.6	n.d.	A	0.025	457	462
16-1, 115	141.2	0.75	E	0.013	679	478
16-2, 45	142	n.d.	D	0.077	93	471
16-3, 45	143.6	n.d.	A	0.021	673	469
17-1, 45	150	n.d.	A	0.042	443	464
17-1, 115	150.6	n.d.	A	0.056	306	470
17-2, 115	151.4	0.67	A	0.030	516	468
Hole 615						
3-2, 72	14.32	n.d.	E	0.012	1002	475 ± 1.4
3-2, 93	14.53	n.d.	n.d.	0.12	45	455 ± 0
6-4	43.6	n.d.	E	0.019	783	467 ± 1
9-1, 77	68.0	n.d.	A	0.025 ± 0.006	474 ± 11	471 ± 7
9-3, 0–2	70.2	n.d.	A	0.053	276	478 ± 5
Hole 618A						
1-2, 13	10.83	n.d.	B	0.028	500	480 ± 2.8
Hole 619						
1-2, 13	2.63	n.d.	A	0.048	401	468 ± 3.5
Hole 621						
21-1	131	0.86	n.d.	n.d.	n.d.	n.d.

[a] See Figure 2.
[b] ng hydrocarbon per mg ash wt.
[c] n.d. = not determined.

data points. At 85 m, the large error bar for P_2 suggests an increase in organic matter heterogeneity. From 95 to 125 m sub-bottom, the P_2 values undergo a second increase, very similar in magnitude and slope to that found in the 40–85 m interval. Below 125 m, a second drop in P_2 occurs and much more scatter is found in the P_2 values from the deeper samples.

The hydrocarbons evolved during pyrolysis were also trapped and the concentrations of individual pyrolysis products measured. This analysis has been carried out for Site 623 sediments as shown by the different capillary GC P_2 patterns (A through E) of pyrolyzed organic matter shown in Figure 4; these patterns correspond to the different symbols shown in Figure 3. The total C_7 to C_{25} compound P_2 depth profile (shown as "tot. cap." in Fig. 3) is almost identical in shape and the concentrations are almost equal to the total pyrolysis P_2 values (which represent C_1 to about C_{32}) described above. Therefore, most of the hydrocarbons evolved in the cracking process are in the C_7–C_{25} range rather than in the gas (C_1–C_6) range, because these lighter compounds are not trapped and analyzed by the capillary GC. The lack of the light hydrocarbon generation potential implies that the organic matter in these sediments, while being fairly lean in terms of hydrocarbon-generating potential, is more prone to oil than to gas generation (Dembicki et al., 1983). This indicates that these sediments do not contain a large proportion of immature terrigenous woody organic matter, which tends to be more gas (methane) prone (Tissot and Welte, 1978; Hunt, 1979).

Two intervals show approximately linear increases in P_2 with depth (from 40 to 85 m and 95 to 125 m sub-

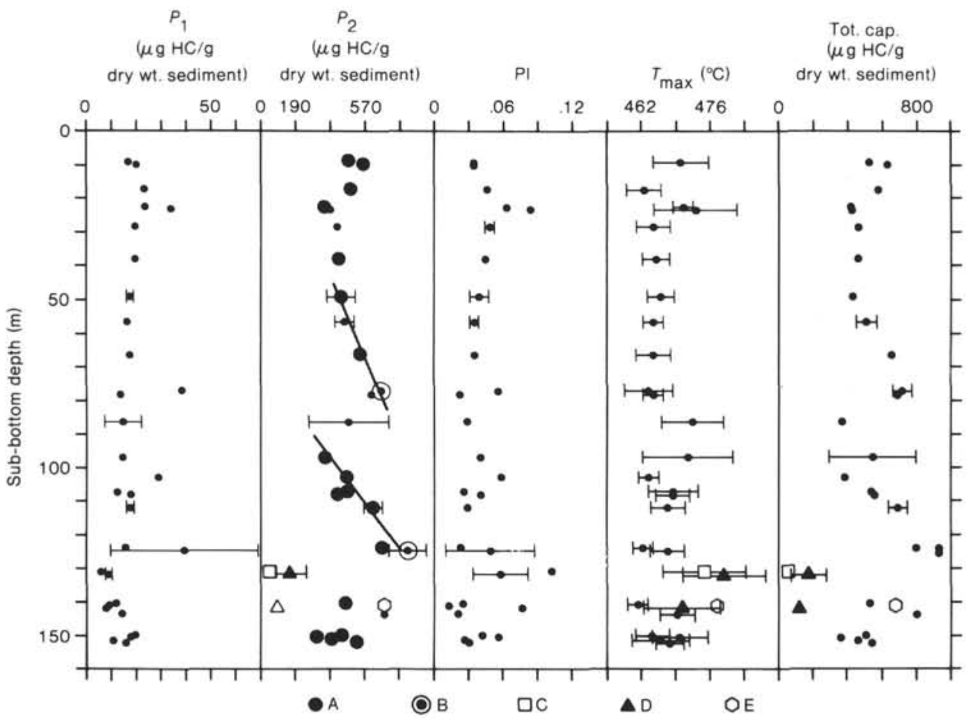

Figure 3. Pyrolysis data for DSDP Leg 96, Site 623. Letters (A-E) and corresponding symbols refer to different organic carbon types identified by typical P_2 capillary GC patterns as shown in Figure 4. Tot. cap. is total capillary GC P_2 values.

bottom). Preliminary shipboard data (lithology and gamma-ray logs) suggested that these intervals might be two "fining upward" sequences of channel–overbank deposits—from 65 to 83 m and from 92 to 120 m sub-bottom. However, sedimentological and well-logging data suggest that complex interbedding of channel-fill and overbank sequences make it difficult to distinguish these sequences on the lower fan sites such as 623. A trend of increasing P_2 with depth within a fining-upward channel–overbank sequence would not be expected. If P_2 values are correlatable with organic carbon content, as has been observed for some immature marine sediments (Whelan and Hunt, 1982; Jasper et al., 1984), then P_2 values would be expected to be higher for the fine-grained sediments at the top of the sequence than for the coarser grained sediments at the bottom, as is generally observed for redeposited organic carbon.

In deeper sections of Site 623 from 126 to 160 m sub-bottom, P_2 values show more scatter and no apparent trend with depth (Fig. 3). The capillary GC patterns of these pyrolysis products also show more scatter in organic carbon types in this part of the hole as compared to shallower sections (Fig. 4). For example, types A and B in Figure 4 appear to have very similar compositions, with B being richer. Note that the richer type B organic matter appears at the bottom of both the postulated channel–overbank sequences (Samples 623-9-2, 43 cm and 623-14-3, 50 cm at 75.7 and 124.9 m, respectively). However, the deeper 126–156 m section contains leaner P_2 types C and D as well as a richer type E. Note that the richer type, E, is very similar to that found in Sections 615-3-2 and 615-6-4 (F and G in Fig. 4). The predominant organic matter type at Site 623, type A in Figure 4, is also seen in two samples from Site 615 (Samples 615-9-1, 77 cm, Fig. 4H, and 615-9-3, 0–2 cm at 68 and 70.2 m, respectively) as well as in the surface section of one of the basin sites (Sample 619-1-2, 13 cm). The capillary P_2 GC pattern of pyrolyzed organic matter in a surface section of a more anoxic basin site, Sample 618A-1-4, 130 cm (Fig. 5I), is richer than A and closely resembles type B (the type detected at the bottom of the two postulated channel–overbank sequences, as discussed above).

The scatter in organic matter types in the deepest sections of this hole also correlates with generally higher and broader T_{max} values (Fig. 3). In petroleum source rocks, the more hydrogen-rich sediment samples just above or entering the petroleum-generation zone give a sharp T_{max} (generally in the range of 480–520°C on the CDS instrument used in this work) with the width of the peak, as shown by the error bars, being in the range of 2–5°C maximum. The T_{max} values then generally increase with depth and show a broader temperature range as petroleum is generated and the remaining pyrolyzable groups become more difficult to break off. A broad T_{max} can also indicate a mixture of organic carbon types, resulting in a mixture of reworked and unreworked material.

The T_{max} values for the Site 623 samples are low and show a broad peak range (Fig. 3) as might be expected for somewhat organic-lean immature sediments containing organic matter from more than one source. The broadness of the T_{max} peaks and the scatter in the values is much more pronounced in the deepest section (126–156 m sub-bottom) suggesting an increased complexity in organic sources—consistent with increased complexity of P_2 capillary GC patterns (as discussed above).

Paleontological data can be used together with the pyrolysis data to constrain the possible organic sources. Below 40 m sub-bottom, planktonic fauna are rare. Most of those present are reworked Cretaceous benthic foraminifers (see Site 623 chapter, this volume), consistent with our relatively low P_2 values which indicate the presence of reworked organic matter. Radiolarians are found in the 0–40 m section, suggesting deposition of marine material and generally lower sedimentation rates. The pyrolysis data do not show a clear difference between the 0–40 m as compared to the 40–160 m interval sediment, although there is possibly a trend to slightly higher P_2 and T_{max} values in the surface sections. The sediments from 126 to 156 m sub-bottom were not analyzed in detail by the paleontologists, so there is no paleontological data to test our hypothesis of more mixed organic sources for this deeper section.

Interpretation of Lower Fan Sites 623 and 615 Pyrolysis Results

Sedimentological data suggest that complex interbedding of channel-fill and overbank sequences may be typical of lower fan sites and that interpretation of the two P_2 increases at Site 623 as channel-fill sequences is an oversimplification. Reexamination of the pyrolysis data taking this complexity into account provides the following information:

1. Some process(es) of unknown nature are causing an overall increase (preservation?) of pyrolyzable organic matter within the depth intervals from 40 to 85 m and from 95 to 125 m sub-bottom.
2. The nature (but not the amount) of high molecular weight organic matter (as determined by pyrolysis capillary GC—Figs. 3, 4) remains fairly constant throughout the hole, except in sections below 125 m. This result implies either that the source of high molecular weight organic matter remains the same but is delivered in varying amounts throughout the hole (which seems unlikely), or that processes (biological?) reworking the sediment organic matter during deposition have remained fairly constant (which seems more likely based on lipid biomarker data—from many geographic areas—Ourisson et al., 1984).

Based on the very limited set of midfan overbank and channel-fill test samples described previously (Table 1), ranges (to be tested in future work) can be proposed for P_2 as related to depositional setting in fan sequences. For immature sediments containing only mud and silt and T_{max} values in the range of 462-468°C (indicating absence of lignite and/or more mature types of carbon), P_2 values of less than 500 μg hydrocarbon per g dry weight sediment are suggested to be typical of channel-fill sequences, while P_2 values greater than 600 represent overbank deposits, slumps, or turbidites. Furthermore, because very low P_2 values occur for sands (<300 μg/g and often <100), it is suggested that sections containing sand which also show very high P_2 values (>500) have been mixed with finer-grained unreworked organic-rich sediments. Such mixing might be expected from debris flows and might also result from drilling disturbance. Slumps or turbidites were postulated to be the cause of abnormally high P_2 values in some Leg 95 sediments (Tarafa et al., in press). Using these criteria, the sediments from lower fan Sites 615 and 623 can be classified as channel-fill (CF), overbank (OB), or slumps (labeled S, includes turbidites) on the basis of pyrolysis as shown in Table 4. It will be interesting to test in future work whether these classifications are realistic in terms of other geological parameters.

CONCLUSIONS

The conclusions reached from pyrolysis analyses of Leg 96 sediments can be summarized as follows:

1. For fan depositional environments, limited and preliminary data suggest that P_2 values of less than 500 μg/g are typical of channel fills; values of greater than 600 μg/g are typical of overbank, slump, or turbidite deposits with the highest values occurring in the latter two types.
2. Microbiological degradation of sedimentary organic matter caused a decrease in P_2.
3. The quantity of pyrolyzable organic matter at fan sites is generally low with values in some basin sections being somewhat higher. The production index and P_1 values are low with respect to petroleum generation and are not typical of sediments containing migrated hydrocarbons.
4. Capillary GC analyses of the pyrolyzable organic matter shows the type (but not the amounts) to be very similar at lower fan Site 623 from 0 to 126 m sub-bottom. Higher yields of pyrolyzable organic matter are postulated to correlate with depositional history. Specifically, more rapid deposition of organic matter would provide less opportunity for oxic biodegradation of sediment organic matter in the water column assuming bottom-water oxygen conditions remained constant.
5. The composition of pyrolysis products suggests an organic matter type that is more prone to oil than to gas generation. This implies that the immature organic matter in these sediments does not contain a significant quantity of woody terrigenous material.
6. T_{max} values are very constant for most sediments. The generally low, broad T_{max} peaks suggest the presence of immature organic matter, possibly reworked by biogenic processes, before deposition. Elevated T_{max} values appear to occur in samples containing lignite.
7. P_2 capillary GC patterns from samples taken from the bottom sediments of Site 623 (126–156 m sub-bottom) show a mixture of organic matter types.
8. Most of the organic matter types found at Site 623, as identified by pyrolysis capillary–GC of P_2 could also be detected at other Leg 96 sites from which data were available at time of this writing (i.e., from Site 615 on the lower fan, and Sites 618 and 619 located in the intraslope basins).
9. A decrease in P_2, which occurs in deeper sections of Basin Site 619, may be related to an increase in terrigenous material and/or to increased bioturbation.

ACKNOWLEDGMENTS

We thank the crew and staff of DSDP for samples, Christine Burton and Joan Brazier for organic carbon analyses, Richard Sawdo for keeping our instruments running, and John Farrington for his helpful comments about the manuscript. K. Peters and an anonymous review-

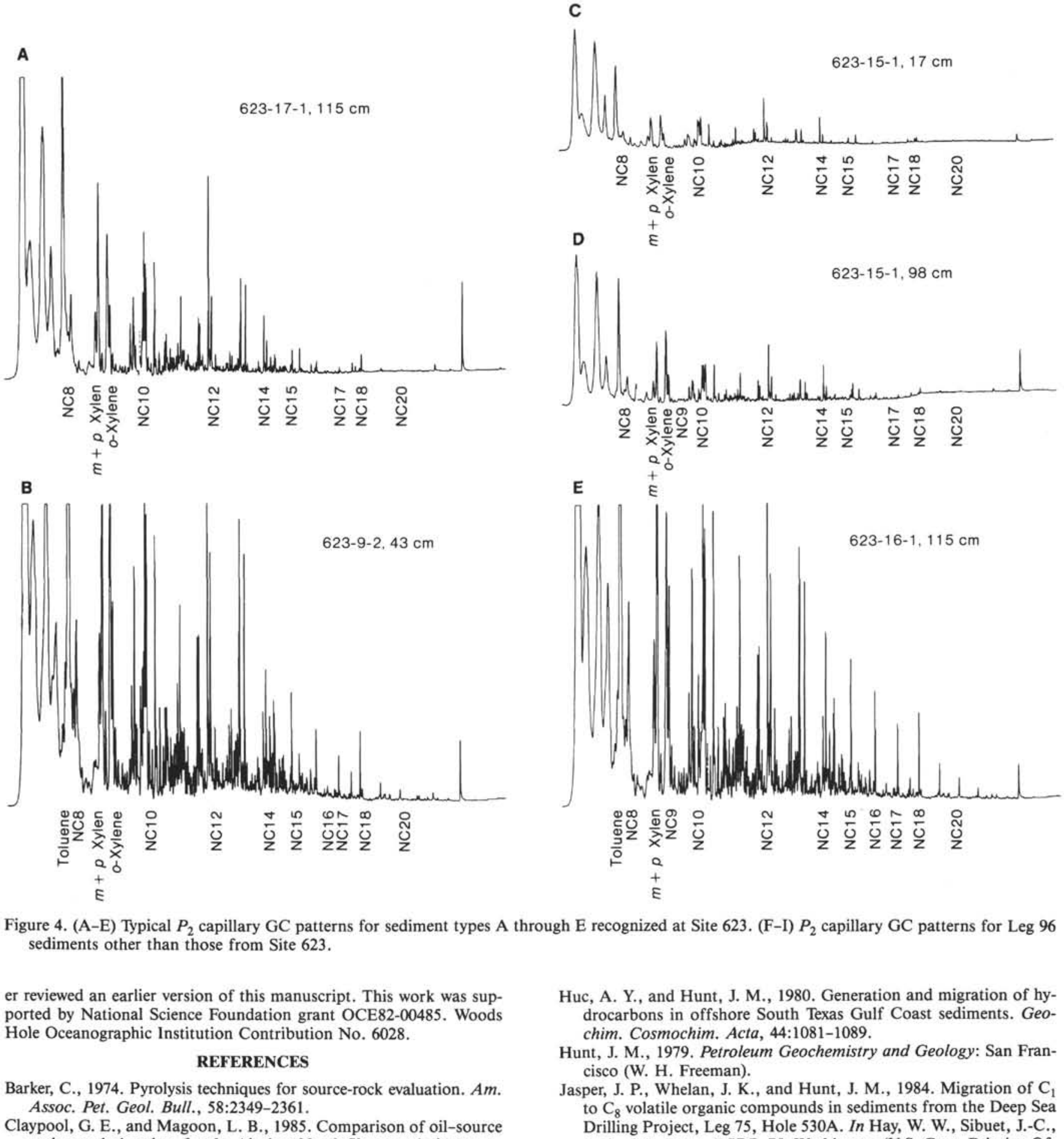

Figure 4. (A–E) Typical P_2 capillary GC patterns for sediment types A through E recognized at Site 623. (F–I) P_2 capillary GC patterns for Leg 96 sediments other than those from Site 623.

er reviewed an earlier version of this manuscript. This work was supported by National Science Foundation grant OCE82-00485. Woods Hole Oceanographic Institution Contribution No. 6028.

REFERENCES

Barker, C., 1974. Pyrolysis techniques for source-rock evaluation. *Am. Assoc. Pet. Geol. Bull.*, 58:2349–2361.

Claypool, G. E., and Magoon, L. B., 1985. Comparison of oil-source rock correlation data for the Alaskan North Slope: techniques, results, and conclusions. *In* Magoon, L. B., and Claypool, G. E. (Eds.), *Alaska North Slope Oil/Source Rock Correlation Study.* Am. Assoc. Pet. Geol., Spec. Stud. Geol., 20:49–81.

Claypool G. E., and Reed, P. R., 1976. Thermal-analysis technique for source-rock evaluation: quantitative estimate of organic richness and effects of lithologic variation. *Am. Assoc. Pet. Geol. Bull.*, 60:608–626.

Dembicki, H., Jr., Horsfield, B., and Ho, T. T. Y., 1983. Source rock evaluation by pyrolysis-gas chromatography. *Am. Assoc. Pet. Geol. Bull.*, 67:1094–1103.

Espitalié, J., Madec, M., Tissot, B., Mennig, J. J., and Leplat, P., 1977. Source rock characterization method for petroleum exploration. *Proc. Annu. Offshore Technol. Conf.*, 9(3):439–444.

Huc, A. Y., and Hunt, J. M., 1980. Generation and migration of hydrocarbons in offshore South Texas Gulf Coast sediments. *Geochim. Cosmochim. Acta*, 44:1081–1089.

Hunt, J. M., 1979. *Petroleum Geochemistry and Geology*: San Francisco (W. H. Freeman).

Jasper, J. P., Whelan, J. K., and Hunt, J. M., 1984. Migration of C_1 to C_8 volatile organic compounds in sediments from the Deep Sea Drilling Project, Leg 75, Hole 530A. *In* Hay, W. W., Sibuet, J.-C., et al., *Init. Repts. DSDP*, 75: Washington (U.S. Govt. Printing Office), 1001–1008.

Ourisson, G., Albrecht, P. A., and Rohmer, M., 1984. The microbial origin of fossil fuels. *Scient. Amer.*, 251(8):44–51.

Tarafa, M. E., Whelan, J. K., and Mountain, G. S., in press. Sediment slumps in the middle and lower Eocene of Deep Sea Drilling Project Holes 605 and 613: Chemical detection by pyrolysis techniques. *In* Poag, C. W., Watts, A. B., et al., *Init. Repts. DSDP*, 95: Washington (U.S. Govt. Printing Office).

Tissot, B. P., and Welte, D. H., 1978. *Petroleum Formation and Occurrence*: Berlin (Springer-Verlag).

Whelan, J. K., Fitzgerald, M. G., and Tarafa, M., 1983. Analysis of organic particulates from Boston Harbor by thermal distillation-pyrolysis. *Environ. Sci. Tech.*, 17:292–298.

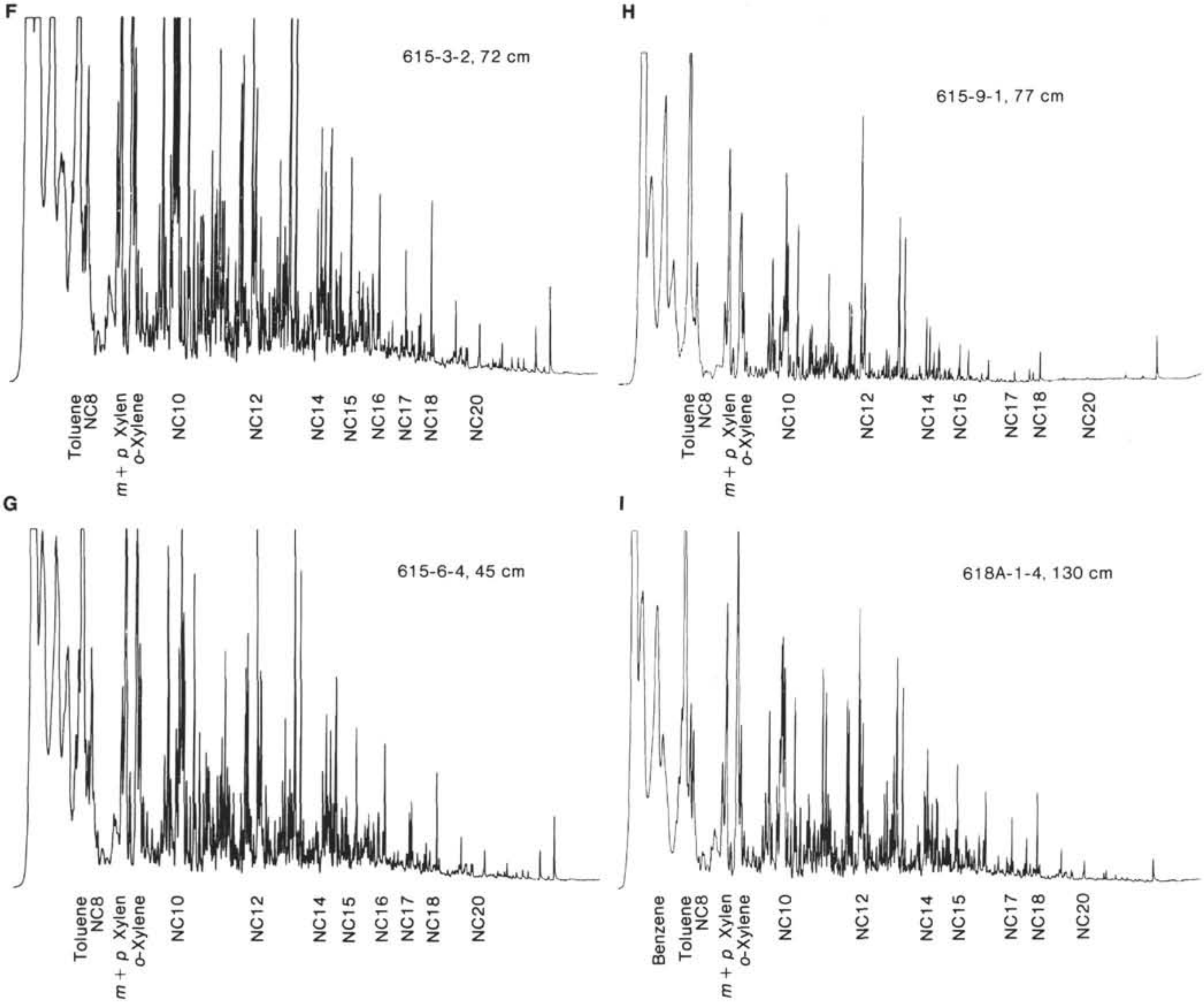

Figure 4. (Continued).

Whelan, J. K., and Hunt, J. M., 1982. Organic matter in Deep Sea Drilling Project Site 504 and 505 sediments studied by a thermal analysis-gas chromatography technique. *In* Cann, J. R., Langseth, M. G., Honnorez, J., Von Herzen, R. P., White, S. M., et al., *Init. Repts. DSDP*, 69: Washington (U.S. Govt. Printing Office), 443-450.

Whelan, J. K., Hunt, J. M., Jasper, J., and Huc, A., 1984. Migration of C_1-C_8 hydrocarbons in marine sediments. *Org. Geochem.*, 6: 683-694.

Date of Initial Receipt: 4 March 1985
Date of Acceptance: 6 September 1985

Table 4. Prediction of channel-fill (CF) versus overbank (OB) versus turbidite or slump (S) deposits based on pyrolysis data.

Core-Section (level or interval in cm)	Sub-bottom depth (m)	P_2 (μg/g)[a]	T_{max} (°C)	Description of sediment	Predicted[b] type
Hole 615					
3-2, 30–33	13.90	640	463	Mud with silt laminae	OB or S
3-2, 70–77	14.30	600	470	Dark grey sandy silt — laminated	S
3-2, 72	14.32	1002	475	Dark grey sandy silt — laminated	S
3-2, 93	14.53	45	455	Dark grey sandy silt — laminated	CF
3-3, 8–9	15.18	57	454	Silty sand — fining upward sequence?	CF
3-3, 63	15.73	624	463	Silty mud	OB or S
5-3, 99–100	33.59	63	464	Silty sand	CF
5-4, 40	34.50	241	470	Mud with deformed silty layers	CF
6-4	43.60	783	467	Dark grey silt — sand (drilling disturbance)	OB or S
6-5, 120	46.30	700	463	Muddy silt — fine-grained turbidites?	OB or S
6-6, 10	46.70	139	464	Sorted silty sand	CF
9-1, 77	68.00	474	471	Silty laminated mud	CF
9-3, 0–2	70.20	276	478	Silty sand	CF
10-1, 10	76.80	700	461	Silty mud	OB or S
10-1, 58	77.28	177	470	Silty sand (with chert; lignite)	nd
33-1, 46	305.16	770	468	Silty turbidite mud	S
47-2, 42	458.62	600	471	Silty mud in layers with lignite	OB or S
49-1, 2–3	485.22	440	467	Nannofossil ooze (homogeneous)	Marine
50-1, 3-4	494.73	575	467	Nannofossil ooze	Marine
51-1, 5–6	504.25	600	465	Foraminifer nannofossil ooze	Marine
Hole 623					
2-2, 115	9.2	479	470	Mottled mud with minor silt laminae	CF
2-3, 45	10.0	556	469	Mottled mud with less color banding	?
3-1, 115	16.2	485	462	Mottled, no bands — silt scour bases	CF
3-5, 45	22.6	351	470	Mottled, no bands — scour bases	CF
5-2, 115	38.0	425	465	Mottled — faint color banding	CF
6-3, 115	49.2	440	466	Dark grey mud, silt laminae	CF
8-2, 69	66.4	545	464	Mud with silt laminae, color bands	?
9-2, 43	75.7	662	464	Interbedded mud and silt	OB or S
10-3, 3–6	86.4	481	472	Contorted mud and dark grey silt	CF
11-3, 1–3	97.0	350	472	Homogeneous mud with silt blebs	CF
12-1, 1–3	103.0	471	464	Dark grey mud with silt laminae	CF
12-4, 17	107.3	473	468	Dark grey mud with silt laminae	CF
12-4, 110	108.2	423	468	Dark grey mud with silt laminae	CF
13-1	112.2	614	468	Deformed mixture silt, sand and mud	S
14-2, 98	123.9	664	462	Color-banded dark grey mud with silt laminae	OB or S
14-3, 50	124.92	805	468	Color-banded/dark grey mud/between two sand layers	OB or S
15-1, 17	131.0	51	475	Dark grey silt — drilling disturbance	CF
15-1, 98	131.8	161	479	Dark grey silt — drilling disturbance	CF
16-1, 45	140.6	457	462	Dark grey mud with silt-sand laminae	CF
16-1, 115	141.2	679	478	Massive dark grey silt	OB or S
16-2, 45	142.0	93	471	Massive dark grey silt	CF
16-3, 45	143.6	673	469	Dark grey mud with silty-sand laminae	S
17-1, 45	150.0	443	464	Dark grey mud — drilling disturbance	CF
17-1, 115	150.6	306	470	Dark grey mud — drilling disturbance	CF
17-2, 115	151.4	516	468	Dark (no sand?) — drilling disturbance	?

[a] μg hydrocarbon per g dry wt. sediment.
[b] OB = overbank; S = slump or turbidite; CF = channel-fill. "Marine" means sediment probably deposited under more marine rather than fan depositional conditions. ? means not classifiable on basis of P_2.